

# Fractional quantum Hall effect at $\nu = 5/2$ : Ground states, non-Abelian quasiholes, and edge modes in a microscopic model

Xin Wan

*Zhejiang Institute of Modern Physics, Zhejiang University, Hangzhou 310027, P.R. China*

Zi-Xiang Hu

*Zhejiang Institute of Modern Physics, Zhejiang University, Hangzhou 310027, P.R. China and  
National High Magnetic Field Laboratory, Tallahassee, Florida 32306, USA*

E. H. Rezayi

*Department of Physics, California State University Los Angeles, Los Angeles, California 90032, USA*

Kun Yang

*National High Magnetic Field Laboratory and Department of Physics,  
Florida State University, Tallahassee, Florida 32306, USA and  
Zhejiang Institute of Modern Physics, Zhejiang University, Hangzhou 310027, P.R. China  
(Dated: February 9, 2022)*

We present a comprehensive numerical study of a microscopic model of the fractional quantum Hall system at filling fraction  $\nu = 5/2$ , based on the disc geometry. Our model includes Coulomb interaction and a semi-realistic confining potential. We also mix in a three-body interaction in some cases to help elucidate the physics. We obtain a phase diagram, discuss the conditions under which the ground state can be described by the Moore-Read state, and study its competition with neighboring stripe phases. We also study quasihole excitations and edge excitations in the Moore-Read-like state. From the evolution of the edge spectrum, we obtain the velocities of the charge and neutral edge modes, which turn out to be very different. This separation of velocities is a source of decoherence for a non-Abelian quasihole/quasiparticle (with charge  $\pm e/4$ ) when propagating at the edge; using numbers obtained from a specific set of parameters we estimate the decoherence length to be around four microns. This sets an upper bound for the separation of the two point contacts in a double point-contact interferometer, designed to detect the non-Abelian nature of such quasiparticles. We also find a state that is a potential candidate for the recently proposed anti-Pfaffian state. We find the speculated anti-Pfaffian state is favored in weak confinement (smooth edge) while the Moore-Read Pfaffian state is favored in strong confinement (sharp edge).

## I. INTRODUCTION

Fractional quantum Hall (FQH) liquids are remarkable many-electron systems that possess nontrivial topological order.<sup>1</sup> Such topological order is reflected in experimental measurable quantities, including the (fractional) charge and statistics angle of the gapped quasiparticle/quasihole excitations supported by the system, and the spectra of gapless edge excitations. By now a large number of different FQH states, usually labeled by a Landau level (LL) filling factor  $\nu = N_e/N_\phi$  (where  $N_e$  is the number of electrons and  $N_\phi$  the number of flux quanta enclosed in the system), have been observed experimentally. Most of these FQH states are the Laughlin states or their hierarchy descendents. These are Abelian FQH states whose quasiparticles obey Abelian fractional statistics, and their edge excitations are made of chiral bosonic modes. The quasiparticle charge has been measured in some of these states,<sup>2</sup> and measurement of the statistics angle has been attempted recently.<sup>3</sup> Edge excitations of such FQH states have also been probed using electron tunneling<sup>4</sup> and other methods.

Recently much interest and attention have focused on a special FQH state with filling factor  $\nu = 5/2$ , first observed twenty years ago.<sup>5</sup> Interest in this system is driven in part by numerical work<sup>6,7</sup> that suggests the Moore-Read Pfaffian state<sup>8</sup> is likely realized in the half-filled first excited Landau level (1LL) at this filling factor.<sup>9</sup> The Moore-Read state is qualitatively different from the Laughlin states and their descendents, in that it is a non-Abelian FQH state, whose quasiparticles obey non-Abelian statistics<sup>10</sup> and whose edge excitations include a branch of *fermionic* mode.<sup>1,11</sup> It has been suggested that non-Abelian quasiparticles can be used for topological quantum computation,<sup>12,13,14,15,16</sup> further fueling the interest in this system. It is known that the Pfaffian state is not particle-hole symmetric. It was pointed out very recently<sup>17,18</sup> that the particle-hole transformed Pfaffian state, termed the anti-Pfaffian state, is also a contender at  $\nu = 5/2$ . These two states are closely related, but different in important ways that have experimental consequences. While the electron-electron interaction is particle-hole symmetric when projected onto a half-filled LL, which suggests these two states would be degenerate if this were the only term present in the microscopic Hamiltonian, in reality the degeneracy between the Pfaffian and anti-Pfaffian states is lifted by terms that break particle-hole symmetry. These

include LL mixing<sup>17,18</sup> and, as we will show later, confining potential.

In this paper we report results of a numerical study of the half filled 1LL in a disc geometry. Our study is complementary to earlier numerical works based on the sphere<sup>6</sup> and torus<sup>7</sup> geometries, because the disc is the only geometry that allows one to study edge states and the closely related physics associated with a confining potential. Our results can be briefly summarized as follows. By varying both the electron-electron interaction and confining potential, various types of ground states are stabilized. We find that the Moore-Read Pfaffian and possibly the anti-Pfaffian ground states are realized in different regions of the parameter space of our model. Within our model they appear to be separated by an intermediate state that we interpret as a stripe state. We further study the quasihole and edge excitations of the Pfaffian state, and show that they indeed have the properties predicted by theory. Furthermore, we are able to extract the velocities of the Pfaffian edge modes, which are of importance in addressing both qualitative and quantitative issues that arise in experimental studies of the edge states,<sup>19</sup> especially those involving quasiparticle tunneling in a double point-contact interferometer.<sup>20,21,22,23,24,25</sup> Some of our results were briefly reported in an earlier letter.<sup>26</sup>

The rest of the paper is organized in the following way. We describe our microscopic model and its Hamiltonian (a mixture of Coulomb interaction and three-body interaction) in Sec. II. In Sec. III we study various competing ground states, which emerge as the lowest energy states in the exact diagonalization study. In Sec. IV we discuss the trapping of charge  $+e/4$  quasiholes by local potentials (generated by, say, an atomic force microscope tip) in certain ground states which are supposed to be in the same universality class as the Moore-Read state. We then discuss the evolution of the edge spectrum with the variation of interaction in Sec. V; in particular, we provide an estimate of the charge and neutral velocities in a real system based on our model, and discuss the implication in the decoherence in double point-contact interference experiments. In Sec. VI we demonstrate the non-Abelian nature of a charge  $+e/4$  quasihole by comparing the edge spectra of a system with and without the quasihole. Potential instability in the fermionic edge mode is found. In Sec. VII, we discuss a potential candidate that emerged from the numerical calculations for the recently proposed anti-Pfaffian state, and speculate on its stability conditions. We summarize our results in Sec. VIII. We leave the technical details of the identification of edge states in a system with mixed three-body and Coulomb interaction to Appendix A. The detailed analysis of the evolution of edge states in the pure Coulomb limit is presented in Appendix B.

## II. THE MICROSCOPIC MODEL

We consider a microscopic model of a two-dimensional electron gas (2DEG) confined to a two-dimensional disk, with a mixed Hamiltonian

$$H = \lambda H_{3B} + (1 - \lambda) H_C. \quad (1)$$

Here, the parameter  $\lambda$  interpolates smoothly between the limiting cases of a purely three-body Hamiltonian  $H_{3B}$  ( $\lambda = 1$ ) and a pure two-body Coulomb Hamiltonian  $H_C$  ( $\lambda = 0$ ). In the following we measure length in units of the magnetic length  $l_B = \sqrt{\hbar c/eB}$  ( $B$  is the magnetic field) and energy in units of  $e^2/\epsilon l_B$  ( $\epsilon$  is the dielectric constant), such that all quantities that appear later are in units of some combination of the two based on their dimensionality.

Explicitly, the three-body interaction  $H_{3B}$  has the form

$$H_{3B} = - \sum_{i < j < k} S_{ijk} [\nabla_i^2 \nabla_j^2 (\nabla_i^2 + \nabla_j^2) \delta(\mathbf{r}_i - \mathbf{r}_j) \delta(\mathbf{r}_i - \mathbf{r}_k)], \quad (2)$$

where  $S$  is a symmetrizer:  $S_{123}[f_{123}] = f_{123} + f_{231} + f_{312}$ , where  $f$  is symmetric in its first two indices. The  $N$ -electron Pfaffian state proposed by Moore and Read<sup>8</sup> for a half-filled lowest Landau level (0LL)

$$\begin{aligned} & \Psi_{MR}(z_1, z_2, \dots, z_N) \\ &= \text{Pf} \left( \frac{1}{z_i - z_j} \right) \prod_{i < j} (z_i - z_j)^2 \exp \left\{ - \sum_i \frac{|z_i|^2}{4} \right\} \end{aligned} \quad (3)$$

is the exact zero-energy ground state of  $H_{3B}$  with the smallest total angular momentum  $M_0 = N(2N - 3)/2$ . In Eq. (3), the Pfaffian is defined by

$$\text{Pf} M_{ij} = \frac{1}{2^{N/2} (N/2)!} \sum_{\sigma \in S_N} \text{sgn} \sigma \prod_{k=1}^{N/2} M_{\sigma(2k-1)\sigma(2k)} \quad (4)$$

for an  $N \times N$  antisymmetric matrix with elements  $M_{ij}$ . In reality, three-body interaction is present due to finite Landau level mixing. The three-body Hamiltonian also has other zero-energy states, known as the edge states, which will be discussed in Sec. V. We note that while the Moore-Read Pfaffian wave function Eq. (3) is written for electrons in the 0LL, it is straightforward to generate the corresponding wave function for electrons in the 1LL by applying the LL raising operator to every electron. For the rest of the paper we will use the 0LL version of various wave functions to simplify our discussion, with the understanding that the 1LL version of the wave function is generated the same way.

However, there is a more transparent formulation of the three-body Hamiltonian in terms of projection operators,<sup>27</sup> which can be written as

$$H_{3B} = \sum_M \sum_{i < j < k} |\psi_M(i, j, k)\rangle \langle \psi_M(i, j, k)|, \quad (5)$$

where  $\psi_M(i, j, k)$  is a three-particle wave function specified below [Eq. (6)] and  $M$  is the total angular momentum of the state. The Hamiltonian for three particles produces a single non-zero eigenvalue which is unity (provided sufficient number of orbitals are allowed) as a true projection operator should. This is the most natural way to define the scale of the three-body Hamiltonian. It is simpler to analyze  $\psi_M$  for bosons first. The corresponding expression for fermions, as usual, is obtained by multiplication of an appropriate Jastrow factor. The Moore-Read wave function for bosons contains one unit of relative angular momentum in the Laughlin factor for each pair, instead of two for fermions. As a result when three particles are brought together the relative angular momentum is  $2 = 3 \times 1 - 1$  (instead of  $5 = 3 \times 2 - 1$ ). We now need to project out all relative angular momenta smaller than two. In this case, the only possibility is angular momentum zero (see Ref. 27 for details). The relative wave function is thus a constant. The total angular momentum  $M$  will have to be absorbed by the center of mass wave function, which is  $(z_1 + z_2 + z_3)^M$ . For fermions the normalized wave function is:

$$\psi_M(z_1, z_2, z_3) = B_M (z_1 + z_2 + z_3)^{M-3} J(z_1, z_2, z_3), \quad (6)$$

where  $J(z_1, z_2, z_3) = (z_1 - z_2)(z_1 - z_3)(z_2 - z_3)$ , and the normalization factor is:

$$B_M = \frac{1}{(2\pi)^{3/2}} \sqrt{\frac{3^{M-4}}{2^{M+2}(M-3)!}}. \quad (7)$$

The total angular momentum of the Jastrow factor  $J$  is 3 and that of the center of mass is  $M - 3$ , giving a total angular momentum  $M$ .

The three-body interaction  $H_{3B}$  has a rather simple form in the occupation space:

$$H_{3B} = \sum_{m_1 > m_2 > m_3} \sum_{m_4 < m_5 < m_6} U(\{m_i\}) \times c_{m_1}^\dagger c_{m_2}^\dagger c_{m_3}^\dagger c_{m_4} c_{m_5} c_{m_6}, \quad (8)$$

and

$$U(\{m_i\}) = V(m_1, m_2, m_3) V(m_4, m_5, m_6), \quad (9)$$

where  $V$  is a completely antisymmetric function of its arguments. With  $M = m_1 + m_2 + m_3$  we have:

$$V(m_1, m_2, m_3) = \sqrt{\frac{(M-1)!}{2 \times 3^M m_1! m_2! m_3!}} A\{m_2 m_1 (m_1 - 1)\}, \quad (10)$$

and  $A$  is the antisymmetrizer in  $m_1, m_2$ , and  $m_3$ . The difference between the spectra of this form of the Hamiltonian and the one with the  $\delta$ -functions is an overall factor of  $\pi^2/8$  in the latter. While there are more efficient ways to obtain the Moore-Read state<sup>28</sup> that avoid diagonalizing a three-body Hamiltonian, here we need the  $H_{3B}$  to generate the spectrum of the mixed three-body and the two-body Coulomb Hamiltonian.

The Coulomb Hamiltonian  $H_C$  includes a two-body Coulomb ( $1/r$ ) interaction and a one-body confining potential provided by the neutralizing background charge distributed uniformly on a parallel disk of radius  $R$ , placed at a distance  $d$  above the 2DEG. This distance parameterizes the strength of the confining potential, which decreases with increasing  $d$ . The rotationally invariant confining potential comes from the Coulomb attraction between the background charge and the electrons. Using the symmetric gauge we can write down the following Hamiltonian for the electrons confined to the 1LL:

$$H_C = \frac{1}{2} \sum_{mnl} V_{mn}^l c_{m+l}^\dagger c_n^\dagger c_{n+l} c_m + \sum_m U_m c_m^\dagger c_m, \quad (11)$$

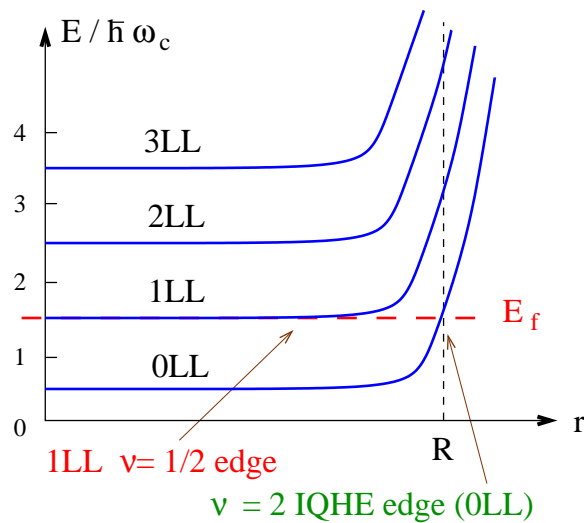


FIG. 1: (color online). Illustration of the edge locations of the  $\nu = 1/2$  Moore-Read state and the  $\nu = 2$  integer quantum Hall state. Although the positive background charge and total electron charge are 5 times that of the electrons forming the Moore-Read state, the edge is hiding behind the integer quantum Hall edge in the lowest Landau level. The Moore-Read edge may thus be protected since it is farther away from the electrostatic edge.

where  $c_m^\dagger$  is the electron creation operator for the first excited Landau level (1LL) single electron state with angular momentum  $m$ .  $V_{mn}^l$ 's are the corresponding matrix elements of Coulomb interaction for the symmetric gauge, and  $U_m$ 's the matrix elements of the confining potential. Additional details of this model can be found in Ref. 29 where we studied edge reconstruction of Abelian fractional quantum Hall states at different  $\nu$ , including explicit expressions of  $U$  and  $V$  and an illustration of the electrostatic configuration associated with  $H_C$  (see Fig. 1 of Ref. 29).

The confining potential we use here is motivated by the  $\delta$ -doping technique in 2DEG fabrication. For GaAs/AlGaAs heterostructures, silicon impurities are deposited in an atomically thick layer at a distance  $d \sim 1000$  Å above the interface where 2DEG is located to reduce impurity scattering. Therefore, we model the background potential arising from these ionized silicon impurities, which ensure charge neutrality in the samples. Even at an electrostatic level it is clear that  $d$  parameterizes the strength of the confining potential. At small  $d$  the potential is strong and also sharp near the edge, while at large  $d$  the potential is weak and smooth near the edge. Alternatively, one may tune the background charge density (right at the 2DEG plane) by smearing out the edge charge density as in an earlier study of edge reconstruction in integer quantum Hall liquids.<sup>30</sup> In the study of Abelian fractional quantum Hall liquids, we find that, e.g., the Laughlin-like state is stable up to  $d \approx 1.5l_B$ , beyond which edge reconstruction takes place.<sup>29</sup> While we expect the parameter  $d$  appropriately characterizes the confining potential, we note the detailed sample structures and fabrication processes have an effect on how realistic the model is.

To study the physics at  $\nu = 5/2$ , we explicitly keep the electronic states in the half-filled 1LL only, while neglecting the spin up and down electrons in the lowest Landau level (0LL), assuming they are inert. The amount of positive background charge is chosen to be equal to that of the half-filled 1LL, so the system is neutral. The choice of a disc radius  $R = \sqrt{4N}l_B$ , where  $N$  is the number of electrons in the 1LL, guarantees that the disk encloses exactly  $2N$  magnetic flux quanta, corresponding to  $\nu = 1/2$  in the 1LL. This is a simplification of the real system. In reality, the background charge equals the *total* electron charge of both the half-filled 1LL and the filled 0LL electrons. The latter neutralizes  $4/5$  of the background charge in the bulk, but this neutralization effect is incomplete near the edge due to finite  $d$ . Furthermore, the location of the 0LL edge is different from that of the 1LL electrons (see Fig. 1). The physical consequences of these effects will be discussed in Section VIII. In this study, we do not consider the finite thickness of the electron layer, which softens the Coulomb interaction and can be studied using the same numerical method, albeit time-consuming.

### III. COMPETING GROUND STATES

Taking advantage of the rotational invariance of the system, we diagonalize the Hamiltonian [Eq. (1)] for each Hilbert subspace with a total angular momentum  $M$ , and correspondingly obtain the ground state energy  $E(M)$ . The global ground state is defined as the ground state with the lowest energy  $E(M_{gs})$ , whose corresponding angular

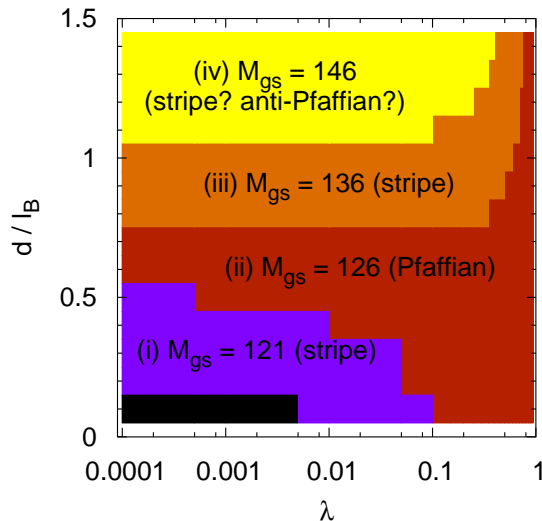


FIG. 2: (color online). Total angular momentum of the global ground state as a function of the mixing parameter  $\lambda$  and background charge distance  $d$  for 12 electrons in 22 orbitals with the mixed Hamiltonian [Eq. (1)]. The ground state in region (ii) has the same  $M_{gs} = 126$  as the Moore-Read (or Pfaffian) wave function. The ground state in regions (i) and (iii) are believed to be stripe phases. In region (iv), the ground state is a candidate for the so-called anti-Pfaffian state (see Sec. VII for detail).

momentum is  $M_{gs}$ . In our approach the ground state angular momentum is a result that comes out of the calculation, rather than a parameter fixed *a priori* based on the property of the state that one is interested in. Therefore, we can *quantitatively* analyze the stability of the ground state.

Figure 2 is a phase diagram that shows the total angular momentum of the global ground state  $M_{gs}$  for 12 electrons in 22 orbitals with the Hamiltonian in Eq. (1). We vary the mixing parameter  $\lambda$  and the background charge distance  $d$ . The Moore-Read state for 12 electrons has  $M_{MR} = N(2N - 3)/2 = 126$ . In the small  $\lambda$  limit, the ground state around  $d = 0.6-0.7$  persist to have  $M_{gs} = 126$ . To be precise, the ground state is stable for  $0.51 \leq d \leq 0.76$  for the pure Coulomb case  $\lambda = 0$ .<sup>26</sup> On the other hand, the range extends as  $\lambda$  increases, since three-body interaction favors the Moore-Read state. The two regions with  $M_{gs} = 121$  and 136 surrounding the Moore-Read ground state are believed to be stripe phases. They can be represented by two strings of 0 and 1's  $|M_{gs} = 121\rangle = |10000011111111110000\rangle$  and  $|M_{gs} = 136\rangle = |110000000111111111000\rangle$ , respectively. The 0 and 1's are the occupation numbers of single-electron angular momentum eigenstates (smaller angular momentum orbitals to the left). Alternatively, one can understand such a string as the Slater determinant of the corresponding single-electron angular momentum eigenstates labeled by 1. At this system size, numerical ground states have an overlap of about 30-40% with the corresponding Slater-determinant states in their range of stability. For very small  $d$  ( $d \approx 0.1l_B$ ),  $M_{gs}$  can jump to 110 for  $\lambda < 0.01$ , which is believed to be a finite-size artifact. On the other hand, there is a region with ground state  $M_{gs} = 146$ , which the authors already showed in Fig. 1b of Ref. 26. Toward the pure Coulomb case, this ground state is stable over a range of  $d$  twice as large as that for the Moore-Read state. We speculate this is related to the so-called anti-Pfaffian state discussed very recently.<sup>17,18</sup> We will discuss this state in greater detail in Sec. VII.

In the absence of three-body interactions, the overlap between the ground state wave function and the Moore-Read wave function,  $|\langle \Psi_{gs}(M_{gs} = 126) | \Psi_{MR} \rangle|^2$ , is about 0.5 for the Coulomb interaction (it jumps up to 0.7 when we tune the  $V_1$  pseudopotential<sup>26</sup>). While this is quite substantial considering the already quite large size of Hilbert subspace, it is significantly smaller compared with the Laughlin state at  $\nu = 1/3$  at comparable system size. Combined with the narrow window of  $d$  within which  $M_{gs} = 126$  in the pure Coulomb interaction case, these suggest that the Moore-Read state may be quite fragile when system parameters are varied. This is consistent with earlier numerical work on the torus<sup>7</sup> and the experimental observation that the FQH state at  $\nu = 5/2$  disappears in a tilted magnetic field for modest tilting angle, even though the state is believed to be spin polarized. We note the phase boundaries in the small  $\lambda$  limit persist in the small negative- $\lambda$  regime ( $-0.02 < \lambda < 0$ ). This suggests the Moore-Read-like ground state with pure Coulomb interaction is stable against a small attractive three-body interaction, which may arise, e.g., due to Landau level mixing.

#### IV. NON-ABELIAN QUASIHOLE WITH ELECTRIC CHARGE $+e/4$ IN THE MOORE-READ STATE

Considering the relatively small overlap and rather narrow window of stability in  $d$ , one might wonder if the  $M_{gs} = 126$  ground state is indeed in the same universality class as the Moore-Read state. To answer this question we must study whether the elementary excitations of this state have the same properties as those of the Moore-Read state. In this section we study the the quasihole excitations of this state by introducing a local potential, possibly induced in experiments by the tip of an atomic force microscope, for example. The next section will be devoted to study of the edge excitations.

As the ground state of the microscopic model is very sensitive to the parameters of the system, such as the background confining potential (by tuning  $d$ ) and the weight ( $\lambda$ ) of the three-body interaction  $H_{3B}$ , one may ask if additional features besides the total angular momentum can offer further support that the ground state is in the same phase as the Moore-Read state. In fact, one of the most striking properties of the Moore-Read state is that it supports charge  $\pm e/4$  quasihole/particle excitations, which carry *half* the charge of a Laughlin quasihole/particle at this filling factor. They obey non-Abelian statistics, and their existence implies that electrons are paired in the ground state (in the same way that observation of  $h/2e$  vortices indicate electrons are paired in superconductors). We note that the Halperin 331 state<sup>31</sup> also supports  $e/4$  charge. But it is a bilayer state with  $1/4$  filling in each layer, thus  $e/4$  charge is not as surprising, as one can get it by threading a flux quantum through one layer only.

In an earlier study,<sup>26</sup> we have demonstrated that a short-range impurity potential at the origin  $H_W = Wc_0^\dagger c_0$  can induce such a fractionally-charged quasihole, in the presence of some three-body potential. In a system of 12 electrons in 24 orbitals (as well as a smaller system of 10 electrons in 20 orbitals), we found for large enough  $W$ , a quasihole of charge  $+e/4$  can appear at the origin. This is reflected in the depletion of  $1/4$  of an electron in the total occupation number of electrons at orbitals with small angular momenta, and in the change of ground state angular momentum from  $M_{gs} = N(2N-3)/2$  to  $N(2N-3)/2 + N/2$ , in agreement with that of the Moore-Read state with the quasihole located at the origin:

$$\begin{aligned} & \Psi_{MR}^{+e/4}(z_1, z_2, \dots, z_N) \\ &= \text{Pf} \left( \frac{z_i + z_j}{z_i - z_j} \right) \prod_{i < j} (z_i - z_j)^2 \exp \left\{ - \sum_i \frac{|z_i|^2}{4} \right\}. \end{aligned} \quad (12)$$

If  $W$  is increased further, a  $+e/2$  quasihole (which is a Laughlin quasihole, equivalent to two  $+e/4$  quasiholes<sup>33</sup>) appears at the origin in the global ground state, whose total angular momentum further increases to  $N(2N-3)/2 + N$ , in agreement with the variational wave function

$$\Psi_{MR}^{+e/2}(z_1, z_2, \dots, z_N) = \left( \prod_i z_i \right) \Psi_{MR}(z_1, z_2, \dots, z_N). \quad (13)$$

In Fig. 3, we show the electron densities of the  $+e/4$  quasihole and the corresponding Moore-Read ground state for 30 electrons obtained by Monte-Carlo simulations. We note that the counterpart of Eq. 12 on the sphere<sup>34</sup> would represent *two*  $+e/4$  quasiholes on the opposite poles of the sphere. In the following, we proceed to explore the existence of the  $+e/4$  quasihole in a larger parameter space, including cases *without* three-body potential ( $\lambda = 0$ ). Since a  $+e/4$  quasihole with Abelian statistics can arise from a strong-pairing state (instead of the weak-pairing Moore-Read state), we will discuss the statistics of the quasihole in Sec. VI after we discuss the edge excitations of the ground state.

We attempt to trap a quasihole at the origin by introducing a Gaussian impurity potential:

$$H_{W,\sigma} = W \sum_m \exp(-m^2/2\sigma^2) c_m^\dagger c_m, \quad (14)$$

where  $\sigma$  (multiplied by  $l_B$ ) is the range of the potential. Note  $H_W = Wc_0^\dagger c_0$  is the short-range limit ( $\sigma \rightarrow 0$ ) of the potential in Eq. 14. Therefore, the additional parameter  $\sigma$  allows us a more complete search. Two of us and a co-worker have also been studying the effect of the range and shape of the potential on the excitation of  $\pm e/3$  quasiholes/quasiparticles in a Laughlin  $\nu = 1/3$  liquid.<sup>32</sup> For  $\sigma \sim 2.0$ , the weakest strength of the Gaussian potential that supports the quasihole state as the global ground state is found insensitive to the confining potential (or  $d$  in our model).<sup>32</sup> In the Moore-Read case, studies also suggest  $\sigma \sim 2.0$  is optimal for the generation of quasiholes, as in its vicinity the quasihole states can remain to be the global ground state even in the pure Coulomb case.

Figure 4 shows the global ground state angular momentum as a function of the mixing parameter  $\lambda$  and the tip potential strength  $W$  for 12 electrons in 22 orbitals, with the mixed Hamiltonian in Eq. (1) and the Gaussian tip potential in Eq. (14). Here, we choose  $d = 0.7l_B$  and  $\sigma = 2.0$ . To be specific, we expect the Moore-Read state with 0,

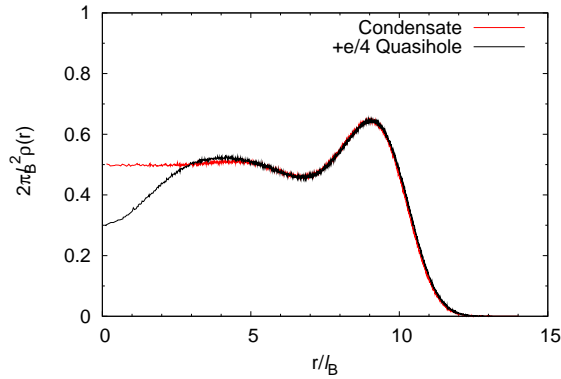


FIG. 3: (color online). The densities of the  $+e/4$  Moore-Read quasihole state (Eq. 12) and the Moore-Read condensate (Eq. 3) for a 30-electron system.

1, and 2 ( $+e/4$ ) quasiholes to have total angular momenta of 126, 132, and 138 respectively. For small  $W$  ( $W < 0.03$ ), we find  $M_{gs} = 126$  for the global ground state, which is the same as the Moore-Read state. When there is enough three-body interaction ( $\lambda > 0.025$ ), as we increase  $W$ ,  $M_{gs}$  first jumps to 132 ( $W > 0.05$ ), and then to 138 ( $W > 0.2$ ) as  $W$  increases; this is exactly what one expects when the system first traps a single  $+e/4$  quasihole, and then two  $+e/4$  quasiholes. However, for smaller  $\lambda$ , there is an additional region with  $M_{gs} = 126$  around  $W = 0.5$ , separating the one-quasihole and two-quasihole regions. This region turns out to be a stripe state, characterized by the binary string |000001111111111100000). Careful analysis suggests that near  $\lambda = 0.025$  and  $W = 0.5$ , the energies of the three states with different total angular momenta are very close to each other and therefore extremely sensitive to the parameters. Despite this complication, we point out that the trapping of a single  $+e/4$  quasihole by a local potential is a robust feature of the ground state, which persists to the pure Coulomb case along the lower boundary ( $W \approx 0.03$ ), at least for finite potential width of  $\sigma = 2.0$ . This strongly suggests that the ground state with  $M_{gs} = 126$  is indeed in the universality class of the Moore-Read state.

We note that a  $\delta$ -function trapping potential ( $\sigma \rightarrow 0$  in our Eq. (14)) was used to generate quasiholes on a sphere by Tóke *et al.*<sup>35</sup> They were unable to isolate individual  $+e/4$  quasiholes for either the pure Coulomb or pure three-body interactions, while in our earlier work<sup>26</sup> we succeeded in doing that on a disc for some mixture of Coulomb and three-body interactions, using the same trapping potential. One advantage of disc geometry is that one can create a *single*  $+e/4$  quasihole in the system, while on a sphere (or torus) such quasiholes must be created in pairs, and their interaction complicates the matter. Here we demonstrate that a single  $+e/4$  quasihole can also be generated and isolated for pure Coulomb interaction, with some finite-range trapping potential. We have not, however, been able to do that with the  $\delta$ -function trapping potential. This suggests that such quasiholes have relatively large size, and its trapping and manipulation will be sensitive to the details of the trapping potential. Thus experimentally one may need to optimize the trapping method in order to generate and manipulate them.

## V. EDGE EXCITATIONS OF THE MOORE-READ STATE AND THE INTERFERENCE EXPERIMENTS

In addition to quasihole/quasiparticle properties, another way to probe the topological order of FQH liquids is to study their edge excitations, which are also of vital experimental importance. For comparison, the Laughlin state supports a single branch of bosonic chiral edge mode, whose properties have been studied in tunneling experiments.<sup>4</sup> For the Moore-Read state, in addition to a bosonic mode whose properties are very similar to that of the Laughlin state, a neutral fermionic branch of excitations has been predicted;<sup>1,11</sup> this fermionic branch is closely related to the non-Abelian nature of the state. The existence of both branches makes the low-energy excitation spectrum of a microscopic model at  $\nu = 5/2$  richer and their experimental consequences more interesting.<sup>36</sup>

In our earlier study,<sup>26</sup> we have observed both branches of modes for a mixed Hamiltonian, and demonstrated that a single  $+e/4$  quasihole in the bulk changes the boundary condition of the fermionic mode, clearly indicating the non-Abelian nature of the quasihole. In this section we provide further details of the analysis of the spectra, and study how the spectra evolve as the interaction is varied, especially toward the pure Coulomb interaction.

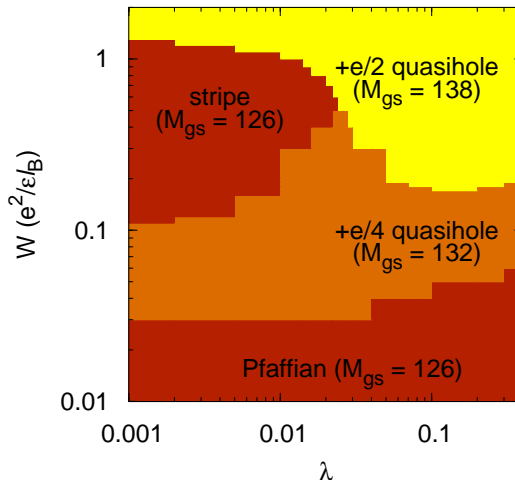


FIG. 4: (color online). Ground state angular momentum as a function of trapping potential and three-body interaction strength. We have 12 electrons in 22 orbitals, with the mixed Hamiltonian [Eq. (1)] and the Gaussian tip potential [Eq. (14)].  $\lambda$  and  $W$  characterize the three-body interaction and tip potential strength respectively. The background charge is fixed at  $d = 0.7l_B$  above the electron layer (the ground state has  $M_{gs} = 126$ , same as the Moore-Read state in the absence of the Gaussian potential). For large enough  $\lambda$ , as the tip potential strength  $W$  increases, states with  $M_{gs} = 132$  or  $M_{gs} = 138$ , believed to contain a  $+e/4$  quasihole or a  $+e/2$  quasihole, become the global ground state. For small  $\lambda$ , another ground state with  $M_{gs} = 126$  (which is a stripe state with occupation pattern  $|0000011111111111100000\rangle$ ), separates these two quasihole states.

#### A. Edge spectrum of a Hamiltonian with mixed electron-electron interaction

In this subsection, we demonstrate a clear separation of the fermionic and bosonic modes for the Moore-Read state, and try to obtain their velocities for  $\lambda = 0.5$ . We will then try to extend the results to the pure Coulomb case in the next subsection. We begin by recalling the procedure to extract edge mode dispersion in the simpler Laughlin case at  $\nu = 1/3$ , where there is only one bosonic branch of edge mode. Then, we apply a similar analysis to the Pfaffian case, where we have a fermionic branch of edge mode in addition to a bosonic one. Of course, unlike the Laughlin case, here we need to rely on several reasonable assumptions, which can be justified *post priori*.

In an earlier work,<sup>29</sup> we studied the energy spectrum of the electron system at  $\nu = 1/3$ , trying to identify the single bosonic branch predicted by the chiral Luttinger liquid theory.<sup>1</sup> The basic idea is that the low-lying excitations of the quantum Hall system at  $\nu = 1/3$  can be described by a branch of single-boson edge states with angular momentum  $l$  ( $l = 1, 2, 3, \dots$ ) and energy  $\epsilon_b(l)$ . Therefore, we can label each low-energy state by a set of (bosonic) occupation numbers  $\{n(l)\}$ , whose total angular momentum is

$$M = M_0 + \Delta M = M_0 + \sum_l n(l)l, \quad (15)$$

and energy

$$E = E_0 + \Delta E = E_0 + \sum_l n(l)\epsilon_b(l), \quad (16)$$

respectively, where  $M_0$  and  $E_0$  are total angular momentum and energy of the corresponding ground state. In Eq. (16) we assumed the interactions between the excitations are negligible, which turns out to be an excellent approximation. Being edge excitations, such states can be independently verified by calculating the squared matrix elements  $T[\{n(l)\}] = |\langle \psi_{\{n(l)\}}(N+1) | c_{3N+\Delta M}^\dagger | \psi_0(N) \rangle|^2$  numerically in the microscopic model, and comparing them with the predictions of the chiral Luttinger liquid theory.<sup>29,37</sup> Note that  $M_0(N+1) - M_0(N) = 3N$  is the difference in total angular momenta between the  $N$ - and  $(N+1)$ -electron ground states. As shown in Ref. 29, even in the presence of background confining potential, the ansatz of Eqs. (15) and (16) can be used to unambiguously identify the bosonic mode energies  $\epsilon_b(l)$ , given that edge excitations are not significantly mixed with bulk excitations. The calculation of  $T[\{n(l)\}]$ , while not necessary, does ensure us the correct identification of these excitations as edge states.

Encouraged by the success of identifying the edge mode dispersion and even predicting the energies of edge excitations in the Laughlin case, we apply the same analysis to the Moore-Read state. The complication is that, in addition

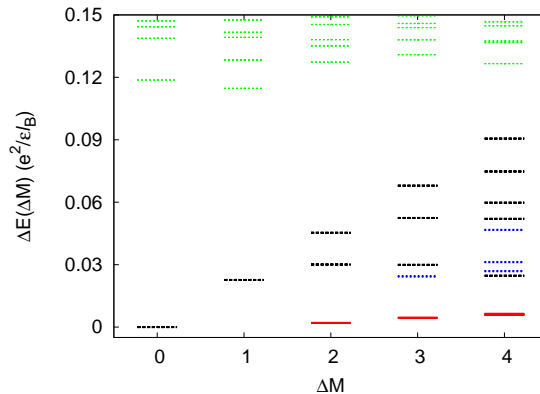


FIG. 5: (color online). Low-energy excitations  $\Delta E(\Delta M)$  from exact diagonalization for  $N = 12$  electrons in 26 orbitals in the 1LL (corresponding to  $\nu = 1/2$ ) for the mixed Hamiltonian in Eq. (1) with  $\lambda = 0.5$ . The neutralizing background charge for the Coulomb part is deposited at  $d = 0.6l_B$  above the electron plane. The red solid bars, the black dashed bars, and the blue dotted bars mark fermionic, bosonic, and mixed edge excitations, respectively (see Appendix A for detail). Bulk excitations are represented by thin dotted bars (green).

to the bosonic mode, we also have a fermionic mode, and thus the convolution of fermionic and bosonic excitations. Figure 5 shows the low-energy excitations  $\Delta E(\Delta M)$  for  $N = 12$  electrons in 26 orbitals in the 1LL for the mixed Hamiltonian with  $\lambda = 0.5$  and  $d = 0.6l_B$ . A gap at around  $\Delta E = 0.1$  is clearly separating the energy spectrum into a low-energy section and a higher-energy one. The numbers of the low-energy states for  $\Delta M = M - M_0 = 0, 1, 2, 3,$  and  $4$  are 1, 1, 3, 5, and 10, respectively, agreeing perfectly with the numbers expected for the Moore-Read state by earlier theoretical work.<sup>1,11</sup> Notably, the lowest two levels for  $\Delta M = 4$  lie very close to each other. Based on the agreement in numbers, we are tempted to call them edge states; but further confirmation comes from the separation and identification of bosonic mode and fermionic mode, as we show below.

We assume each low-energy excitation can be labeled by two sets of occupation numbers  $\{n_b(l_b)\}$  and  $\{n_f(l_f)\}$  for bosonic and fermionic modes with angular momenta  $l_b, l_f$ , and energies  $\epsilon_b, \epsilon_f$ , respectively.  $n_b(l_b)$  are non-negative integers while  $n_f(l_f) = 0, 1$ . Since the fermionic edge excitations are Majorana fermions that obey antiperiodic boundary conditions,<sup>11</sup>  $l_f$  must be positive half integers, while for bosonic mode  $l_b$  are integers. In addition, the total fermion occupation number  $\sum_{l_f} n_f(l_f)$  for each state must be an even integer because each fermionic excitation contains an even number of Majorana fermion modes due to their pairing nature. The angular momentum and energy of the state, measured relatively from those of the ground state, are

$$\Delta M = \sum_{l_b} n_b(l_b)l_b + \sum_{l_f} n_f(l_f)l_f; \quad (17)$$

$$\Delta E = \sum_{l_b} n_b(l_b)\epsilon_b(l_b) + \sum_{l_f} n_f(l_f)\epsilon_f(l_f). \quad (18)$$

The details of the analysis on the data of Fig. (5) are presented in Appendix A. Here we summarize the results in Table I and Fig. 6(a). Interestingly, the fermionic dispersion curve is monotonic and can be well fit by a straight line passing the origin, allowing us to obtain the neutral fermionic velocity  $v_n = d\epsilon_f/dk \approx 0.0016Re^2/(\epsilon l_B \hbar)$ , where the disc radius  $R = 2\sqrt{N}l_B$ , and we have the conversion from the angular momentum to the linear momentum along the edge  $k = \Delta M/R$ . For typical GaAs systems, we obtain  $v_n \approx 2 \times 10^5$  cm/s. On the other hand, in contrast to the roughly linear dispersion of the fermionic branch, the energy of the bosonic branch bends down (despite a much bigger initial slope or higher velocity), suggesting a potential vulnerability to edge reconstruction in the bosonic branch<sup>29,38</sup>. This is not surprising since the bosonic mode is charged; as a result its velocity is dominated by the long-range nature of the Coulomb interaction in the long-wavelength limit, but at the same time it is also more sensitive to the competition between Coulomb interaction and confining potential which can lead to instability at shorter wavelengths. If we assume the curve is linear for  $k \leq 1/R$ , we can estimate  $v_c \approx 3 \times 10^6$  cm/s for GaAs.

Using these  $\epsilon_b$ 's and  $\epsilon_f$ 's (a total of 8 energies), we can re-construct the whole low-energy spectrum of the system up to  $\Delta M = 4$  (a total of 20 states), which agrees well with the actual spectrum<sup>26</sup> (in fact, we can extend the construction to  $\Delta M = 5$  and obtain very satisfactory agreement for most states, which do not involve edge modes with larger momentum). The consistency justifies our analysis based on the assumption that the interactions between excitations are negligible and further supports our central result in this section, namely the fermionic mode is well

$l_b$	$\epsilon_b(l_b)$	$l_f$	$\epsilon_f(l_f)$
1	0.022659	1/2	0.000324
2	0.030057	3/2	0.001676
3	0.029908	5/2	0.004117
4	0.024668	7/2	0.006011

TABLE I: Dispersion energies of both bosonic and fermionic modes at small momenta for  $N = 12$  electrons at half filling (in 26 orbitals) in the first Landau level. The system has a Hamiltonian of 50% Coulomb interaction and 50% three-body interaction. The background charge is placed at  $d = 0.6$ . Based on these energies, we can construct the complete low-energy (edge) spectrum of the 12-electron Pfaffian state up to  $\Delta M = 4$  (Ref. 26).

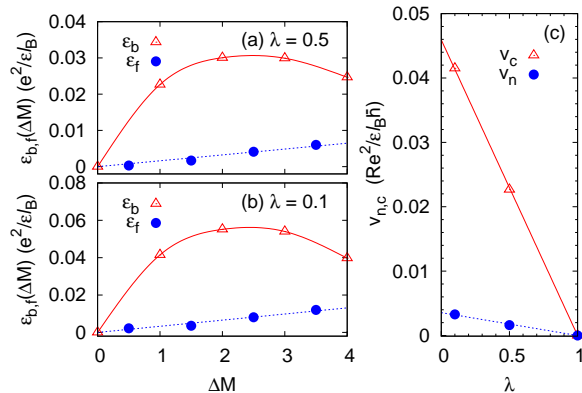


FIG. 6: (color online). (a) Dispersion curves of bosonic ( $\epsilon_b$ ) and fermionic modes ( $\epsilon_f$ ) for  $N = 12$  electrons at half filling (in 26 orbitals) in the first Landau level for  $\lambda = 0.5$ . These energies can be used to construct the complete edge spectrum for the 12-electron system up to  $\Delta M = 4$ .<sup>26</sup> (b) Dispersion curves for the same system with  $\lambda = 0.1$ , or less three-body interaction. (c) Bosonic ( $v_c$ ) and fermionic velocities ( $v_n$ ) extrapolated to the pure Coulomb case. We obtain the  $\lambda = 0.5$  and  $0.1$  points from fitting the fermionic modes to a straight line in (a) and (b), respectively. At  $\lambda = 1$  (pure three body interaction,  $v_n = 0$  as all edge states have zero energies. We thus obtain  $v_c = 0.046$  and  $v_n = 0.0036$ , in units of  $(Re^2)/(e l_B \hbar)$ , for the pure Coulomb case.

separated from the bosonic mode and has much lower energy and velocity.

## B. Toward the pure Coulomb interaction

The ultimate goal of our work is, of course, to understand the low-energy spectrum with pure Coulomb interaction, or at least with less three-body interaction. Looking at the energy spectra for  $\lambda = 0.1$  (Fig. 7) and  $0.0$  (Fig. 8), we fail to observe a gap separating edge and bulk states, as in Fig. 5. One interesting question is, as they start to have similar energies, whether bulk states and edge states are mixed. However, without the gap, it is difficult to identify each eigenstate as a bulk state, a specific edge state, or a mixture of edge and bulk states. To allow the identification, we calculate the overlaps between the eigenstates for  $\lambda = 0.5$ , which we have already analyzed, and the eigenstates for  $\lambda = 0.1$  and  $0.0$ . We assume the eigenstates evolve smoothly as  $\lambda$  decreases, which turns out to be the case as our analysis will show. Thus, we can trace the edge states identified for  $\lambda = 0.5$  and sort them out from all eigenstates in the pure Coulomb case by calculating overlaps; the sorting is otherwise impossible. In particular, we are interested in the evolution of fermionic edge states, which play an important role in understanding the non-Abelian nature of the Moore-Read state.

We leave the details of the approach to Appendix B, but highlight the main results here. We first look at  $\lambda = 0.1$ . Figure 7 shows the low-energy excitations for 12 electrons in 26 orbitals in the 1LL for the mixed Hamiltonian in Eq. (1) with  $\lambda = 0.1$ . The neutralizing background charge for the Coulomb part is deposited at  $d = 0.6l_B$  above the electron plane, just as in the previous case. We find the fermionic edge excitations (red solid bars) are well separated from bulk and other edge excitations, as there is clearly a spectral gap around  $\Delta E = 0.02$ . Another observation is for  $\Delta M = 4$ . Here the two fermionic excitations can be significantly mixed with each other, as the two states for  $\lambda = 0.1$  have roughly equal overlap with the two for  $\lambda = 0.5$ .

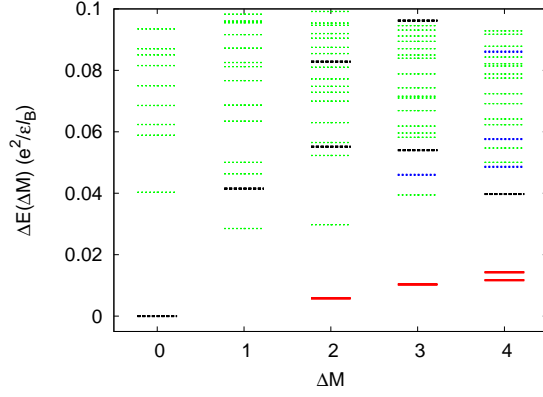


FIG. 7: (color online). Low-energy excitations  $\Delta E(\Delta M)$  from exact diagonalization (solid lines) for  $N = 12$  electrons in 26 orbitals in the 1LL (corresponding to  $\nu = 1/2$ ) for the mixed Hamiltonian in Eq. (1) with  $\lambda = 0.1$ . The neutralizing background charge for the Coulomb part is deposited at  $d = 0.6l_B$  above the electron plane. The red solid bars, the black dashed bars, and the blue dotted bars mark fermionic, bosonic, and mixed edge excitations, respectively. Bulk excitations are represented by thin dotted bars (green). While the bosonic edge excitations mix significantly with the bulk excitations, the fermionic edge excitations are still well separated from the rest (see Appendix B 1 for detail).

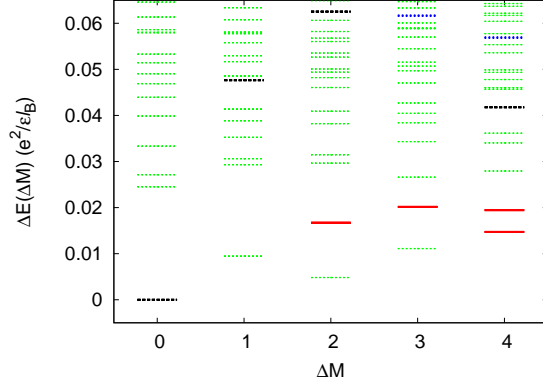


FIG. 8: (color online). Low-energy excitations  $\Delta E(\Delta M)$  from exact diagonalization (solid lines) for  $N = 12$  electrons in 26 orbitals in the 1LL (corresponding to  $\nu = 1/2$ ) for pure Coulomb interaction ( $\lambda = 0.0$ ). The neutralizing background charge for the Coulomb part is deposited at  $d = 0.6l_B$  above the electron plane. The red solid bars, the black dashed bars, and the blue dotted bars mark fermionic, bosonic, and mixed edge excitations, respectively. Bulk excitations are represented by thin dotted bars (green). In this case, fermionic edge excitations also mix with the bulk excitations (see Appendix B 2 for detail).

Similar to what we have done in the previous subsection, we can extract the bosonic and fermionic mode energies for  $\lambda = 0.1$ , plotted in Fig. 6(b). Interestingly, the figure looks exactly like that for  $\lambda = 0.5$ , except the energy scales are roughly doubled for a higher percentage of Coulomb interaction. The bosonic curve bends down slightly further. In this case,  $v_n(\lambda = 0) = 0.0033Re^2/(\epsilon l_B \hbar)$ .

Figure 8 shows the low-energy excitations for pure Coulomb interaction and the confining potential with  $d = 0.6$  for 12 electrons in 26 orbitals. Unfortunately, there is no clear distinction between edge modes and bulk modes at this system size. The situation here is similar to a related study on a rotating Bose gas.<sup>39</sup> After calculating the overlaps, we find the energies of the lowest fermionic edge excitations are around 0.02, but there are lower eigenstates which originate from bulk excitations. We note that a recent DMRG study suggest the bulk gap of the fractional quantum Hall liquid at  $\nu = 5/2$  is approximately 0.03.<sup>40</sup>

Unfortunately, we can no longer extract meaningful results for the bosonic and fermionic dispersion curves for the pure Coulomb interaction as we did for  $\lambda = 0.5$  or 0.1. We believe the reason is that the fermionic mode starts to mix with bulk states, distorting the dispersion curves (see Appendix B for detail). Nevertheless, we can extrapolate the bosonic and fermionic velocities from the two finite- $\lambda$  values, along with the fact that the velocities are zero for the pure three-body case  $\lambda = 1$ , because all edge states have zero energy in  $H_{3B}$ .<sup>11</sup> This also suggests that the velocities should be roughly proportional to the weight of Coulomb interaction  $1 - \lambda$ , which is indeed what we find in Fig. 6(c).

The extrapolations give  $v_c = 0.046$  and  $v_n = 0.0036$  for the pure Coulomb case ( $\lambda = 0$ ), in units of  $Re^2/(\epsilon l_B \hbar)$ . In GaAs systems they are  $v_c \approx 5 \times 10^6$  cm/s and  $v_n \approx 4 \times 10^5$  cm/s, respectively. We can check the validity of the numbers using Fig. 8; for example, the bosonic state at  $\Delta M = 1$  is at  $E = 0.0476$ , very close to 0.046 based on the value of  $v_c$ . Similar comparisons also find  $v_n \approx 0.004(Re^2)/(\epsilon l_B \hbar)$  is in reasonable agreement with the energies at  $\Delta M = 2$  and 3.

We close this subsection by noting that the mixing between bulk and edge excitations seen here for pure Coulomb interaction or small  $\lambda$  is a finite size effect. The edge excitations, which are gapless in the thermodynamic limit, have a finite gap due to the existence of a minimum momentum  $k$  dictated by system size. When this gap is larger than the bulk excitation gap (which is quite small for the Moore-Read-like state with pure Coulomb interaction), mixing between the two types of excitations occurs. They will ultimately separate as system size increases, in the long-wave length limit  $k \rightarrow 0$ . Adding the three-body interaction makes this separation occur at *smaller* system size, by *increasing* the bulk gap without affecting the edge excitation energy much. Thus the effect of adding three-body interaction is similar to increasing system size, which allows us to extract useful information within the accessible system sizes.

### C. Implications on interference experiments

Our numerical calculation suggests that the neutral mode velocity  $v_n$  is much smaller than the charge velocity  $v_c$ . A similar conclusion has been reached in an effective edge theory study, which also suggests the neutral velocity has a dynamic origin.<sup>41</sup> The situation is somewhat similar to what happens in a 1D Luttinger liquid of spin-1/2 electrons, where the velocity of the spin mode is in general lower than that of the charge mode, leading to the so called spin-charge separation. Here we coin a similar term, ‘‘Bose-Fermi separation’’, to describe the separation of the velocities of charged bosonic and neutral fermionic edge excitations of the Moore-Read edge.

In a Luttinger liquid, spin-charge separation is a main source of the decoherence of a single electron<sup>42</sup>. Physically this is because an electron carries both spin and charge; once it enters the Luttinger liquid however, its spin and charge components propagate with different velocities, leading to physical separation between the two after some decoherence time, and loss of integrity of the electron.

The same physics is relevant to the fate of a charge  $\pm e/4$  quasihole/quasiparticle when it is propagating along the Moore-Read edge. A charge  $\pm e/4$  quasihole/quasiparticle carries both a bosonic component and a fermionic component; the former carries its charge while the latter is responsible for its non-Abelian nature. Similar to the case of an electron in a Luttinger liquid, we expect Bose-Fermi separation to be a main source of decoherence of such a non-Abelian quasihole/quasiparticle when it propagates at the edge. This raises a concern that such decoherence may destroy the interference pattern coming from the interference between charge  $\pm e/4$  quasiholes/quasiparticles in interferometry experiments proposed recently.<sup>21,22</sup> In a very recent work,<sup>25</sup> it was found that the decoherence length is indeed very sensitive to the velocities:

$$L_\phi = \frac{1}{2\pi k_B T} \left( \frac{1/8}{v_c} + \frac{1/8}{v_n} \right)^{-1}. \quad (19)$$

As a result, in a double point-contact interferometer, the oscillatory tunneling current due to interference of  $\pm e/4$  quasiholes/quasiparticles decays like  $I \propto e^{-L/L_\phi}$ , where  $L$  is the distance between the two point contacts. It is clear from the equation above that  $L_\phi$  is controlled by  $v_n$ , when  $v_n \ll v_c$ , and smaller  $v_n$  leads to shorter  $L_\phi$ .

Based on our numerical results, we can estimate the constraints on the interferometry experiments due to decoherence. In the pure Coulomb case, we use the bosonic and fermionic velocities extrapolated in Fig. 6(c). Assuming the experiments are done at a temperature of 10 mK and a magnetic field of 5 T,<sup>43</sup> we estimate  $L_\phi \approx 4 \mu\text{m}$ ; this raises concerns on the appropriate inter-point-contact distance  $L$  in interference experiments. In fact, this may be a (perhaps overly) optimistic estimate, as we have not considered the errors due to finite system size and other realistic issues like filled lowest Landau level. Most importantly, the confining potential we use in our model (with parameter  $d/l_B \sim 1$ ) is much stronger than that for real systems;<sup>29,38</sup> real samples have much bigger  $d/l_B$ , resulting in weaker confinement and thus smaller  $v_n$ , leading to a smaller  $L_\phi$  (see next section for further discussion on this point). Thus our estimate using parameters extracted from the specific model we use is best viewed as an upper bound of  $L_\phi$ . Further investigation on this is thus needed.

We close this subsection by noting that while Bose-Fermi separation has important consequences on the decoherence of charge  $\pm e/4$  quasiholes/quasiparticles, it does not affect charge  $\pm e/2$  Laughlin quasiholes/quasiparticles that only carry the Bose component. The interference pattern due to these Laughlin  $\pm e/2$  quasiholes/quasiparticles, unfortunately, does not exhibit the exciting non-Abelian behavior. Thus in interference experiments it is possible that while the interference due to charge  $\pm e/4$  quasiholes/quasiparticles is lost due to decoherence, one can still observe

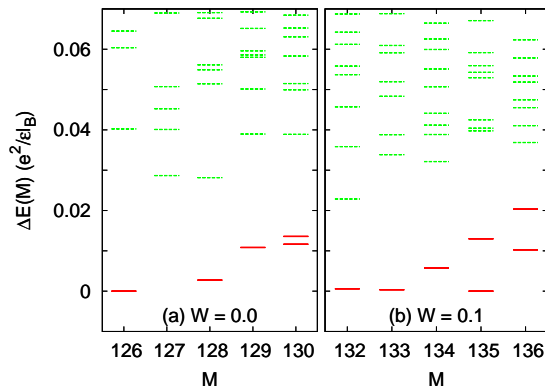


FIG. 9: (color online). Low-energy spectra in a system of 12 electrons in 24 orbitals for the mixed Hamiltonian with  $\lambda = 0.1$  and  $d = 0.7l_B$ . (a) In the absence of the external tip potential, the ground state ( $M = 126$ ) is Moore-Read-like. There are 0, 1, 1, 2 low-energy (fermionic) excitations for  $\Delta M = 1-4$ . (b) In the presence of a Gaussian tip potential ( $W = 0.1$  and  $\sigma = 2.0$ ), the  $+e/4$  quasihole state emerge at  $M = 132$ . There are 1, 1, 2, 2 low-energy (fermionic) excitations for  $\Delta M = 1-4$ . This suggests that a single  $+e/4$  quasihole changes the fermionic mode spectrum. (The states of interest are marked by red solid bars.)

an interference pattern due to charge  $\pm e/2$  quasiholes/quasiparticles, which is similar to that in Laughlin states. In addition to Laughlin quasiholes/quasiparticles, there are also charge  $\pm e/2$  quasiholes/quasiparticles that carry a neutral fermion ( $\psi$ ) but are also Abelian. Bose-Fermi separation does affect their propagation and thus suppresses their interference. Also the added fermion component makes tunneling of such  $\pm e/2$  quasiholes/quasiparticles irrelevant,<sup>36</sup> further reducing their importance.

## VI. NON-ABELIAN NATURE OF $+e/4$ QUASIHOLE AND POSSIBLE INSTABILITY OF FERMIONIC MODE AT THE EDGE

Now armed with the capability of exciting quasiholes as well as the knowledge of edge modes, we are in a position to reveal the non-Abelian nature of a  $+e/4$  quasihole by studying the change of fermionic edge states in the presence of the quasihole. Such a change has been reported in an earlier paper by three of the authors<sup>26</sup> for  $\lambda = 0.5$ ,  $d = 0.5l_B$  and a short-range tip potential. Here we are presenting a case with less three-body interaction ( $\lambda = 0.1$ ), weaker confinement ( $d = 0.7l_B$ ), and a Gaussian tip potential.

Figure 9 shows the low-energy spectra in a system of 12 electrons in 24 orbitals for the mixed Hamiltonian in Eq. (1) with  $\lambda = 0.1$  and  $d = 0.7l_B$ . In the absence of the external tip potential (Fig. 9a), the ground state ( $M = 126$ ) is Moore-Read-like, as we can also read from the phase diagram in Fig. 2 (albeit in 22 orbitals). The excitation spectrum clearly has a gap up to roughly 0.03, consistent with the result from numerical DMRG calculations.<sup>40</sup> Inside the gap, there are 0, 1, 1, 2 low-energy excitations for  $\Delta M = 1-4$  (marked by red solid bars); the numbers agree precisely with the number of fermionic states, as discussed in Sec. V. Comparison with Fig. 7 suggests that the fermionic mode dispersion gets distorted by the increased  $d$  (smoother confinement).

In the presence of a Gaussian tip potential ( $W = 0.1$  and  $\sigma = 2.0$ ), a new ground state emerges at  $M = 132$ , reflecting the fact that a  $+e/4$  quasihole has been trapped by the tip potential. Now there are 1, 1, 2, 2 low-energy (fermionic) excitations for  $\Delta M = 1-4$ . For any  $M$ , there is an energy gap of at least 0.016 separating the fermionic edge states and the rest. The results suggest that a single  $+e/4$  quasihole changes the fermionic mode spectrum, a remarkable feature due to the non-Abelian nature of the  $+e/4$  quasihole. More precisely, a quasihole carries a  $\sigma$  field of the Ising conformal field theory, and its presence changes the boundary condition of the edge Majorana fermion mode from being antiperiodic to periodic. This leads to a shift of the angular momentum quantum numbers of the lowest energy fermionic edge excitations.<sup>11</sup> Since the non-Abelian properties of such quasiholes are exclusively due to the  $\sigma$  degree of freedom it carries, observing such a change of boundary condition directly confirms the non-Abelian nature of the quasihole.

We note that for this particular set of parameters, two of the low-energy fermionic edge states ( $\Delta M = 1$  and 3) actually have very small *negative* energies measured from the single quasihole state with  $M = 132$ . This is sensitive to the choice of parameters; for sharper confinement (with a cutoff of 22 orbitals), the quasihole state *is* the global ground state. This does suggest that there are potential instabilities in the fermionic mode; such possible instabilities and

their consequences remain to be investigated. We note that even if such instabilities do not occur, the closeness of the fermionic excited state energies to zero suggests the neutral velocity can be even smaller with smoother confinement, which can jeopardize the estimate we made in the previous section on the dephasing length relevant to double point-contact interference experiments.

## VII. DISCUSSION ON THE POSSIBLE ANTI-PFAFFIAN STATE

In Sec. III, we mentioned a stable ground state with the same angular momentum quantum number as the recently proposed anti-Pfaffian state.<sup>17,18</sup> In this section, we discuss how this quantum number is determined.

Suppose we have a system of  $N$  electrons in  $N_{orb}$  orbitals. The Pfaffian state, or the Moore-Read state, has a total angular momentum of  $N(2N - 3)/2$ . In order to be able to accommodate this state, we need  $N_{orb} \geq 2N - 2$ . From another angle, we can equivalently view the system as having  $N_h = N_{orb} - N$  holes in  $N_{orb}$  orbitals. The simplest version of the anti-Pfaffian state, by definition, is the Pfaffian state formed by all the holes; this is possible as long as  $N_{orb} \geq 2N_h - 2$ , or  $N_{orb} \leq 2N + 2$ . The total angular momentum (for holes) is thus

$$M_h = \frac{N_h}{2}(2N_h - 3) = \frac{N_{orb} - N}{2}[2(N_{orb} - N) - 3]. \quad (20)$$

The total angular momentum in the original electron basis is

$$M_{AP} = N_{orb}(N_{orb} - 1)/2 - M_h, \quad (21)$$

where the first term is the contribution from the electron background that fully occupies all  $N_{orb}$  orbitals, and the hole contribution  $M_h$  is negative because a hole removes an electron from an occupied orbital. For  $N = 12$  and  $N_{orb} = 22$ , we find  $N_h = 10$ ,  $M_h = 85$ , and  $M_{AP} = 146$ . This is exactly the total angular momentum of the ground state in the region (iv) in Fig. 2. Furthermore we found that increasing the three-body interaction enhances the Pfaffian state and *suppresses* this state; this is consistent with our speculation that this is the anti-Pfaffian state.

This is, however, not definitive evidence, as there are competing states with the same quantum number. In particular, a 12-electron stripe-like state represented by the binary string  $|11000000011111111100\rangle$  has the same angular momentum 146 and very low energy. Analysis of the system with  $N = 12$  electrons in 22 orbitals with pure Coulomb interaction reveals a large overlap (0.35) between the numerical ground state and the stripe state.

We now explore more general possibilities of the anti-Pfaffian state by increasing  $N_{orb}$  from 22 to 24. If the same 10-hole anti-Pfaffian state were to be realized, the two extra holes would be at the two outermost orbitals, and the ground state will have the same quantum number. Stripe or other states, on the other hand, are more likely to respond to the change of boundary. In our numerical calculation, we indeed find the global ground state still has  $M_{tot} = 146$  for  $d = 1.2$ . In addition, the overlap between the ground state and the stripe state discussed above decreases to 0.13. This seems to suggest that the stripe phase is favored by sharp (hard-wall) confinement, as the two outermost orbitals are unoccupied. With smoother confinement, a different state, which we speculate is related to the anti-Pfaffian state, emerges. At  $d = 1.5$ , the ground state momentum increases to 151; this can not be easily explained by a simple stripe phase. On the other hand, it could be explained as the anti-Pfaffian state with one  $+e/4$  quasi-hole.

These findings suggest that, due to the presence of a confining potential, the Pfaffian and anti-Pfaffian states have different energies, and may be realized at different confining potential strengths, *without invoking effects of Landau level mixing*. This is because the confining potential *breaks* the particle-hole symmetry. Based on our model calculation, we speculate that the Pfaffian state is stable as the ground state for strong confinement (sharp edge and smaller  $d$ ), while the anti-Pfaffian state is stable for weak confinement (smooth edge and larger  $d$ ). It is worth pointing out that the two phases are separated and strongly influenced by a stripe phase. Whether this is a generic feature or a finite-size artifact cannot be resolved in the current work. Since the anti-Pfaffian is stable around  $d = 1.5l_B$ , it opens another interesting possibility that edge reconstruction<sup>38</sup> may play a more important role in the anti-Pfaffian state.

## VIII. CONCLUDING REMARKS

To summarize, we have studied a microscopic model of fractional quantum Hall liquids at filling fraction  $\nu = 5/2$ . The interaction between electrons are interpolated continuously between the limits of purely the three-body interaction and purely the Coulomb interaction. Another parameter we vary in our study is the strength of confinement potential, parameterized by the distance  $d$  separating the positive neutralizing background charge and the 2D electron gas layer. This enables us to reveal the nature of ground states and elementary excitations in the pure Coulomb interaction

limit and with semi-realistic confining potential. In particular, we find a Moore-Read-like state is realized in a small window of parameter space, with predicted properties.

The Moore-Read-like ground state has an edge spectrum consistent with that of a charged bosonic mode and a neutral fermionic mode. The fermionic mode has much lower energy than the bosonic mode, implying the neutral velocity is at least an order of magnitude smaller than the charge velocity. This leads to a constraint on the dephasing length for charge  $\pm e/4$  quasiholes/quasiparticles:  $L_\phi < 4 \mu\text{m}$  for typical experimental parameters, at  $T = 10 \text{ mK}$ . This length is of crucial importance in double point-contact interference experiments.

A local potential with a finite width ( $\sim 2l_B$ , or about 20 nm), modeling an atomic force microscope tip, can induce exactly one charge  $+e/4$  quasihole or one charge  $+e/2$  (equivalent to 2 charge  $+e/4$  quasiholes). From the change of fermionic edge mode when a single charge  $+e/4$  quasihole is excited, we confirm the non-Abelian nature of charge  $+e/4$  quasihole.

A ground state with the same quantum number as the recently proposed anti-Pfaffian state is stable in a weak and smooth edge confining potential. The state is found to be separated from the Moore-Read Pfaffian state by a stripe-like state in finite-size calculation.

In the present work, we have used a semi-realistic model for the numerical calculations and attempted to obtain concrete numbers in experimental units, although further improvement is certainly possible and probably necessary. Among the effects we have neglected here, perhaps the most important is the presence of the electrons occupying the lowest Landau level (0LL), and their associated edge (see Fig. 1). These 0LL electrons have two effects that are not included in our study. The first is that the background charge needs to be equal to the *total* electron charge, not just those in 1LL. While the additional charge is neutralized by the 0LL electron charge in the bulk, this neutralization is incomplete at the edge, which results in a fringe electric field<sup>29</sup> that tends to destabilize the 1LL edge through edge reconstruction. On the other hand, due to the cyclotron gap between the 0LL and 1LL, the 1LL edge “hides behind” the 0LL edge, and gets protected from instabilities by the 0LL edge. Thus these two effects that we neglected impact the 1LL edge in opposite ways, and further studies are needed to resolve which effect dominates, and the ultimate fate of the 1LL edge.

Nevertheless we do believe the numbers obtained from the present work can be of use as guidance to experimentalists who are interested in engineering samples and devices or in manipulating individual non-Abelian quasiholes in these devices. The parameters considered here, which describes the smoothness of the edge (related to the location of  $\delta$ -doping in realistic epitaxially grown samples) and the size of an atomic force microscope tip are intimately relevant to experiments. For example, a momentum-resolved magneto-tunneling study has found that an epitaxially overgrown cleaved edge can realize the sharp edge limit.<sup>44</sup> With these realistic issues in mind, this work supports the possibility of topological quantum computing<sup>45</sup> using fractional quantum Hall states, although the road ahead needs further exploration.

An immediate follow-up study, which can strengthen the confirmations found in this work, is the study of the effects of the electron layer thickness, currently under exploration. A recent study by Peterson and Das Sarma<sup>46</sup> claims that finite layer thickness enhances the Moore-Read state, using the criterion of wave function overlap. It would be interesting to study the layer thickness effects in our more sophisticated model using criteria involving ground state energy, bulk and edge excitations. In addition, one also desires to look at the results in larger systems, where finite-size effects are weaker. Techniques to reduce the size of the Hilbert space using various truncation schemes are under development.

## IX. ACKNOWLEDGMENTS

We acknowledge the support from NSFC Grant No. 10504028 (X.W.) and NSF grants No. DMR-0225698, No. DMR-0704133 (K.Y.) and DMR-0606566 (E.H.R.). This research was supported in part by the PCSIRT (Project No. IRT0754) and by the PKIP of CAS. Z.X.H. thanks the CCAST for hospitality during a joint workshop with the KITPC on “Topological Quantum Computing” in Beijing.

## APPENDIX A: ANALYSIS OF EDGE EXCITATIONS AT $\lambda = 0.5$

In this appendix, we discuss in detail the analysis of the edge excitations for the mixed Hamiltonian with  $\lambda = 0.5$ , plotted in Fig. 5. Below  $E = 0.1$ , we have 1, 1, 3, 5, and 10 states with respective angular momenta  $\Delta M = M - M_0 = 0, 1, 2, 3, 4$ , which are well separated from the rest; we identify them as low-energy excitations below the bulk excitation gap. The sequence of numbers are those expected from edge excitations made of a chiral bosonic branch and a chiral fermionic branch. Therefore, we want to associate each of the 20 states with two sets of occupation numbers  $\{n_b(l_b)\}$  and  $\{n_f(l_f)\}$  for bosonic and fermionic modes with angular momenta  $l_b, l_f$ , and energies  $\epsilon_b, \epsilon_f$ , respectively.

$\Delta M = 1$		$\lambda = 0.1 \rightarrow$				
$\downarrow \lambda = 0.5$	1	2	3	4	5	
1	0.017	<u>0.827</u>	0.034	0.001	0.000	
2	0.594	0.048	0.266	0.000	0.004	
3	0.230	0.003	0.470	0.112	0.068	
4	0.004	0.000	0.033	0.361	0.278	
5	0.000	0.056	0.002	0.003	0.026	

TABLE II: Overlap matrix of the two systems with  $\lambda = 0.5$  (row) and 0.1 (column) for  $N = 12$ ,  $N_{orb} = 26$ ,  $M = 127$ , and  $d = 0.6$ . The largest overlap between eigenstates for  $\lambda = 0.1$  and the lowest state (edge state) for  $\lambda = 0.5$  comes from the second lowest state for  $\lambda = 0.1$ , with a value of 0.827 (underlined).

Besides the ground state, it is not difficult to identify the only low-lying state at  $\Delta M = 1$  as the bosonic mode with energy  $\epsilon_b(1) = \Delta E(\Delta M = 1) = 0.022659$ . We can thus identify all edge states at energies  $\Delta E = n_b(1)\epsilon_b(1)$  with corresponding momenta  $\Delta M = n_b(1)$ .

For  $\Delta M = 2$ , we associate the highest-energy state with  $\Delta E \approx 2\epsilon_b(1)$ . There are two more states left, with energies  $\epsilon_b(2)$  and  $\epsilon_f(1/2) + \epsilon_f(3/2)$ . There are thus two choices. However, given  $\epsilon_b(1) \approx 0.02$ , it is reasonable to assume  $\epsilon_b(2) = 0.030057$  is the higher one of the two. As a result, the fermionic state with the smallest momentum has much lower energy than the bosonic ones. Counting the energy states with nearly zero energy (or to be more precise, with  $\Delta E < 0.01$ ), we find 0, 1, 1, and 2 states for  $\Delta M = 1, 2, 3$ , and 4, respectively. These numbers agree perfectly with the results expected for a single branch of Majorana fermion mode.<sup>1,11</sup> We thus assume these energies are sums of two Majorana fermion energies. For  $\Delta M = 2$ , for example, we have already assumed  $\Delta E = \epsilon_f(1/2) + \epsilon_f(3/2)$  for the only state.

For  $\Delta M = 3$ , we have five states. We continue to assume that the lowest one is a purely fermionic state with  $\Delta E = \epsilon_f(1/2) + \epsilon_f(5/2)$ . We can also identify two bosonic states with energies  $\Delta E = 3\epsilon_b(1) \approx 0.066$  and  $\epsilon_b(1) + \epsilon_b(2) \approx 0.052$ . We also find one more from the convolution of both bosonic and fermionic modes with energy  $\Delta E = \epsilon_b(1) + \epsilon_f(1/2) + \epsilon_f(3/2) \approx 0.024$ . The edge state left should then be the bosonic state with  $\Delta E = \epsilon_b(3) = 0.029908$ .

The situation becomes more complicated at  $\Delta M = 4$ , where we have two fermionic, five bosonic, and three convoluted edge excitations. It is easy to identify the convoluted excitations first, at energies  $\epsilon_b(1) + \epsilon_f(1/2) + \epsilon_f(5/2)$ ,  $\epsilon_b(2) + \epsilon_f(1/2) + \epsilon_f(3/2)$ , and  $2\epsilon_b(1) + \epsilon_f(1/2) + \epsilon_f(3/2)$ . Using  $\epsilon_b(l)$  for  $l = 1-3$  obtained above, we can identify four bosonic states at energies  $4\epsilon_b(1)$ ,  $2\epsilon_b(1) + \epsilon_b(2)$ ,  $2\epsilon_b(2)$ , and  $\epsilon_b(1) + \epsilon_b(3)$ . The only state with energy  $\Delta E > 0.01$  is thus the remaining bosonic state with  $\epsilon_b(4) = 0.024668$ . Once again, the two fermionic states have much smaller energy  $\Delta E = \epsilon_f(1/2) + \epsilon_f(7/2)$  and  $\epsilon_f(3/2) + \epsilon_f(5/2)$ . We note that in order to write down a variational wave function for a pair of Majorana-Weyl fermions with momenta  $l > k$ , we need at least  $(2N + l - 1)$  orbitals. Therefore, by reducing the Hilbert space by using fewer orbitals, the hard-wall edge confinement will increase some fermionic mode energies, but leave others intact. This is a test that can unambiguously distinguish the two states. In particular,  $\epsilon_f(7/2)$  will suffer from an energy increase when we reduce the total number of orbitals to 25, while  $\epsilon_f(5/2)$  will remain roughly unchanged unless we further reduce the orbital number to 24 and below. We have observed this confinement effect in numerical calculations, which suggests the state with energy  $\epsilon_f(3/2) + \epsilon_f(5/2)$  is the lower of the two. This energy, together with the two fermionic excitations at smaller momenta, allow us to solve  $\epsilon_f(1/2)$ ,  $\epsilon_f(3/2)$ , and  $\epsilon_f(5/2)$ . Consequently, the energy of the other state [ $\epsilon_f(1/2) + \epsilon_f(7/2)$ ] allows us to solve for  $\epsilon_f(7/2)$ . The results are summarized in Table I and Fig. 5.

Interestingly, the fermionic dispersion curve is smooth, monotonic and can be well fit by a straight line passing the origin, allowing us to obtain the neutral fermionic velocity  $v_n$ . The bosonic dispersion curve, on the other hand, is non-monotonic and bends downward, which indicates a tendency toward edge reconstruction.<sup>38</sup> A very similar analysis can be performed for  $\lambda = 0.1$ , which we leave out for brevity. The results are compared with  $\lambda = 0.5$  in Fig. 6.

## APPENDIX B: NUMERICAL ANALYSIS OF THE EVOLUTION OF EDGE EXCITATIONS

### 1. $\lambda = 0.1$

We discuss here in detail how we identify the edge excitations in Fig. 7 by calculating the overlaps between eigenstates for different  $\lambda$ . Let us start with the simplest nontrivial case  $\Delta M = 1$  (Table II). The lowest excitation (state #1) for  $\lambda = 0.5$  has the largest overlap (0.827, underlined) with the second excitation (state #2) for  $\lambda = 0.1$ . Meanwhile,

$\Delta M = 2$		$\lambda = 0.1 \rightarrow$				
$\downarrow \lambda = 0.5$	1	2	3	4	...	12
1	<u>0.910</u>	0.013	0.001	0.000	...	0.000
2	0.000	0.011	0.169	<u>0.638</u>	...	0.000
3	0.000	0.000	0.000	0.000	...	<u>0.730</u>
4	0.002	0.753	0.001	0.033	...	0.000
5	0.003	0.021	0.464	0.104	...	0.013

TABLE III: Overlap matrix of  $\lambda = 0.5$  (row) and  $0.1$  (column) for  $N = 12$ ,  $N_{orb} = 26$ ,  $M = 128$ , and  $d = 0.6$ . The underlined numbers are the overlap between an edge state for  $\lambda = 0.5$  and the (likely) corresponding edge state for  $\lambda = 0.1$ .

$\Delta M = 3$		$\lambda = 0.1 \rightarrow$				
$\downarrow \lambda = 0.5$	1	2	3	4	...	20
1	<u>0.910</u>	0.001	0.000	0.000	...	0.000
2	0.000	0.000	<u>0.895</u>	0.005	...	0.001
3	0.000	0.185	0.004	<u>0.524</u>	...	0.001
4	0.000	0.000	0.000	0.000	...	<u>0.351</u>
5	0.000	0.000	0.000	0.000	...	0.000

TABLE IV: Overlap matrix of  $\lambda = 0.5$  (row) and  $0.1$  (column) for  $N = 12$ ,  $N_{orb} = 26$ ,  $M = 129$ , and  $d = 0.6$ . The underlined numbers are the overlap between an edge state for  $\lambda = 0.5$  and the (likely) corresponding edge state for  $\lambda = 0.1$ .

state #1 for  $\lambda = 0.1$  has large overlaps with states #2 and #3 for  $\lambda = 0.5$ , both bulk excited states. Therefore, we can identify  $(\Delta M, \Delta E) = (1, 0.0415)$  (state #2 for  $\Delta M = 1$ ) as an edge state for  $\lambda = 0.1$ , with an overlap of 0.827 with the corresponding edge state #1 for  $\lambda = 0.5$ .

For  $\Delta M = 2$ , we find that states #1, #4, and #12 have significant overlaps with the lowest three edge states for  $\lambda = 0.5$ , as listed in Table III. As in Fig. 7,  $\Delta E(\#12, \Delta M = 2) = 0.0828$  is roughly the sum of two  $\Delta E(\#2, \Delta M = 1) = 0.0415$ . This simple addition law resembles the one we have found for edge states at one of the Laughlin filling fractions  $\nu = 1/3$ ,<sup>29</sup> reflecting the conservation of energy and angular momentum.

We may assume, based on this observation, that  $\Delta E(\Delta M = 3) = 3\Delta E(\#2, \Delta M = 1)$  is an edge state (not plotted in Fig. 7). The other four edge states for  $\Delta M = 3$  are found, by comparing overlaps, to be states #1, #3, #4, and #20, according to Table IV. We note the approximate equalities  $\Delta E(\#20, \Delta M = 3) \approx \Delta E(\#2, \Delta M = 1) + \Delta E(\#4, \Delta M = 2)$  and  $\Delta E(\#3, \Delta M = 3) \approx \Delta E(\#2, \Delta M = 1) + \Delta E(\#1, \Delta M = 2)$ .

Similarly, we can identify six edge excited states in the lowest 20 eigenstates we have calculated for  $\Delta M = 4$ . In addition, we can postulate the existence of another four edge states with excitation energies of  $4\Delta E(\#2, \Delta M = 1)$ ,  $2\Delta E(\#2, \Delta M = 1) + \Delta E(\#4, \Delta M = 2)$ ,  $2\Delta E(\#4, \Delta M = 2)$ , and  $\Delta E(\#2, \Delta M = 1) + \Delta E(\#4, \Delta M = 4)$ , respectively. Again, the simple conservation law seems to work fairly well. We point out that the two fermionic edge states (#1 and #2), whose energies are close, mix significantly with each other with respect to the  $\lambda = 0.5$  case. To a lesser extent, another two states (#3 and #4) also mix with each other.

$\Delta M = 4$		$\lambda = 0.1 \rightarrow$					
$\downarrow \lambda = 0.5$	1	2	3	4	5	6	7
1	<u>0.491</u>	<u>0.420</u>	0.001	0.000	0.001	0.000	0.002
2	<u>0.402</u>	<u>0.503</u>	0.004	0.001	0.001	0.002	0.005
3	0.002	0.001	<u>0.565</u>	0.194	0.053	0.002	0.008
4	0.000	0.000	0.121	<u>0.327</u>	0.177	0.222	0.028
5	0.002	0.000	0.000	0.004	0.050	0.114	<u>0.562</u>

TABLE V: Overlap matrix of  $\lambda = 0.5$  (row) and  $0.1$  (column) for  $N = 12$ ,  $N_{orb} = 26$ ,  $M = 130$ , and  $d = 0.6$ . The underlined numbers are the overlap between an edge state for  $\lambda = 0.5$  and the (likely) corresponding edge state for  $\lambda = 0.1$ .

$\Delta M = 1$	$\lambda = 0.0 \rightarrow$							
$\downarrow \lambda = 0.5$	1	2	3	4	5	6	7	8
1	0.003	0.000	0.001	0.012	0.008	0.006	<u>0.403</u>	0.019
2	0.309	0.281	0.007	0.047	0.004	0.012	0.006	0.007
3	0.222	0.025	0.104	0.113	0.013	0.038	0.000	0.000
4	0.007	0.036	0.103	0.034	0.012	0.170	0.000	0.001
5	0.000	0.000	0.002	0.000	0.003	0.001	0.140	0.008

TABLE VI: Overlap matrix of the two systems with  $\lambda = 0.5$  (row) and  $0.0$  (column) for  $N = 12$ ,  $N_{orb} = 26$ ,  $M = 127$ , and  $d = 0.6$ . The underlined element of  $0.403$  is the overlap of the lowest state (edge state) for  $\lambda = 0.5$  (mixed system) and the seventh lowest state for  $\lambda = 0.0$  (pure Coulomb system).

$\Delta M = 2$	$\lambda = 0.0 \rightarrow$					
$\downarrow \lambda = 0.5$	1	2	3	4	...	17
1	0.187	<u>0.432</u>	0.070	0.000	...	0.000
2	0.003	0.001	0.000	0.000	...	<u>0.168</u>
3	0.000	0.000	0.000	0.000	...	0.000
4	0.288	0.206	0.003	0.019	...	0.007
5	0.005	0.015	0.006	0.187	...	0.000

TABLE VII: Overlap matrix of  $\lambda = 0.5$  (row) and  $0.0$  (column) for  $N = 12$ ,  $N_{orb} = 26$ ,  $M = 128$ , and  $d = 0.6$ . The underlined numbers are the overlap between an edge state for  $\lambda = 0.5$  and the (likely) corresponding edge state for the pure Coulomb case.

## 2. The pure Coulomb case

We now move to the pure Coulomb case with  $\lambda = 0$  and look for the eigenstates with significant overlap with the edge states in the  $\lambda = 0.5$  system. Surprisingly for  $\Delta M = 1$ , the 7th lowest state has the largest overlap with the bosonic eigenstate in the corresponding subspace for  $\lambda = 0.5$  (Table VI). The overlap  $0.403$  is far from unity, but comparable to that between the Pfaffian state and the ground state of the pure Coulomb system. The six lower eigenstates (with the notable exception of the state #5), which have negligible overlaps with the edge state, have nonetheless significant overlaps with the lowest energy bulk excited states 2-5 for  $\lambda = 0.5$ , indicating their bulk nature. The complexity of the Coulomb case is thus evident even for the  $\Delta M = 1$  case.

The attempt to find all edge states, even with the overlap matrix calculation, is challenged by the following two difficulties. First, the edge states now have very large excitation energies, and thus a lot more eigenstates are needed for the search. Second, the overlaps with eigenstates for  $\lambda = 0.5$  fail to exhibit a clear one-to-one correspondence. In many cases, an edge states for  $\lambda = 0.5$  can have comparable overlaps with two eigenstates for  $\lambda = 0$ , making the identification ambiguous. Despite the difficulties, we can identify a number of edge states with some confidence.

We end the Appendix by making several observations. First, at this relatively small system size, bulk excited states can have energies as low as those of edge states. In fact, the lowest energy eigenstates for  $\Delta M = 1-3$  are

$\Delta M = 3$	$\lambda = 0.0 \rightarrow$					
$\downarrow \lambda = 0.5$	1	2	3	4	...	17
1	0.220	<u>0.301</u>	0.095	0.004	...	0.004
2	0.000	0.000	0.001	0.002	...	<u>0.361</u>
3	0.012	0.014	0.003	0.001	...	0.001
4	0.000	0.000	0.000	0.000	...	0.001
5	0.000	0.000	0.000	0.000	...	0.000

TABLE VIII: Overlap matrix of  $\lambda = 0.5$  (row) and  $0.0$  (column) for  $N = 12$ ,  $N_{orb} = 26$ ,  $M = 129$ , and  $d = 0.6$ . The underlined numbers are the overlap between an edge state for  $\lambda = 0.5$  and the (likely) corresponding edge state for the pure Coulomb case.

$\Delta M = 4$	$\lambda = 0.0 \rightarrow$						
$\downarrow \lambda = 0.5$	1	2	3	4	5	6	7
1	<u>0.252</u>	<u>0.250</u>	0.004	0.003	0.008	0.005	0.088
2	<u>0.284</u>	<u>0.240</u>	0.029	0.001	0.029	0.000	0.013
3	0.002	0.000	0.029	0.005	0.045	<u>0.093</u>	0.003
4	0.001	0.000	0.019	0.000	0.023	0.005	0.000
5	0.004	0.000	0.000	0.001	0.001	0.000	0.001

TABLE IX: Overlap matrix of  $\lambda = 0.5$  (row) and  $0.0$  (column) for  $N = 12$ ,  $N_{orb} = 26$ ,  $M = 130$ , and  $d = 0.6$ . The underlined numbers are the overlap between an edge state for  $\lambda = 0.5$  and the (likely) corresponding edge state for the pure Coulomb case.

bulk states, with small but finite overlaps ( $\sim 0.2$ ) with the corresponding edge states (see Tables VI, VII and VIII). This suggests in the pure Coulomb case fermionic edge states mix with bulk states, which is consistent with the fact that fermionic edge states extrapolated from finite- $\lambda$  neutral velocities are expected at energies in between the corresponding lowest two levels for  $\Delta M = 2$  and  $3$  (see Fig. 8). A recent density-matrix renormalization group (DMRG) calculation<sup>40</sup> estimate the excitation gap to be about  $0.03 e^2/\epsilon l_B$ , thus we expect these bulk states will float up in the thermodynamic limit. Second, the low-lying fermionic edge excitations do exist for  $\lambda = 0$  at small excitation energies. However, we cannot easily decompose these states into Majorana fermionic levels with linear dispersion relation as we have done for  $\lambda = 0.5$  and  $0.1$ . The difficulty is due to mixing of the fermionic edge excitations with bulk states. Third, there is significant redistribution in the weight of the lowest two edge excitations for  $\Delta M = 4$  as  $\lambda$  decreases, as indicated by the overlaps of the two states for  $\lambda = 0.1$  and  $0.0$  with those for  $\lambda = 0.5$  (see Tables V and IX).

- 
- <sup>1</sup> X.-G. Wen, Adv. Phys. **44**, 405 (1995).  
<sup>2</sup> V. J. Goldman and B. Su, Science **267**, 1010 (1995); L. Saminadayar, D. C. Glattli, Y. Jin and B. Etienne, Phys. Rev. Lett. **79**, 2526 (1997); R. de-Picciotto, M. Reznikov, M. Heiblum, V. Umansky, G. Bunin and D. Mahalu, Nature (London) **389**, 162 (1997).  
<sup>3</sup> F. E. Camino, W. Zhou, and V. J. Goldman, Phys. Rev. B **72**, 075342 (2005).  
<sup>4</sup> A. M. Chang, Rev. Mod. Phys. **75**, 1449 (2003).  
<sup>5</sup> R. L. Willett, J. P. Eisenstein, H. L. Stormer, D. C. Tsui, A. C. Gossard, and J. H. English, Phys. Rev. Lett. **59**, 1776 (1987).  
<sup>6</sup> R. H. Morf, Phys. Rev. Lett. **80**, 1505 (1998).  
<sup>7</sup> E. H. Rezayi and F. D. M. Haldane, Phys. Rev. Lett. **84**, 4685 (2000).  
<sup>8</sup> G. Moore and N. Read, Nucl. Phys. B **360**, 362 (1991).  
<sup>9</sup> A working assumption here is that the lowest Landau level has been fully occupied by both up- and down-spin electrons, and this accounts for filling factor 2; the remaining electrons with filling factor 1/2 occupy the first excited Landau level.  
<sup>10</sup> C. Nayak and F. Wilczek, Nucl. Phys. B **479**, 529 (1996).  
<sup>11</sup> M. Milovanović and N. Read, Phys. Rev. B **53**, 13 559 (1996).  
<sup>12</sup> A. Kitaev, Ann. Phys. **303**, 2 (2003).  
<sup>13</sup> M. H. Freedman, A. Kitaev, and Z. Wang, Commun. Math. Phys. **227**, 587 (2002).  
<sup>14</sup> M. H. Freedman, M. Larsen, and Z. Wang, Commun. Math. Phys. **227**, 605 (2002).  
<sup>15</sup> S. Das Sarma, M. Freedman, and C. Nayak, Phys. Rev. Lett. **94**, 166802 (2005).  
<sup>16</sup> N. E. Bonesteel, L. Hormozi, and G. Zikos, and S. H. Simon, Phys. Rev. Lett. **95**, 140503 (2005).  
<sup>17</sup> S.-S. Lee, S. Ryu, C. Nayak, and M. P. A. Fisher, Phys. Rev. Lett. **99**, 236807 (2007).  
<sup>18</sup> M. Levin, B. I. Halperin, and B. Rosenow, Phys. Rev. Lett. **99**, 236806 (2007).  
<sup>19</sup> J. B. Miller, I. P. Radu, D. M. Zumbuhl, E. M. Levenson-Falk, M. A. Kastner, C. M. Marcus, L. N. Pfeiffer, and K. W. West, Nature Physics **3**, 561 (2007).  
<sup>20</sup> E. Fradkin, C. Nayak, A. Tsvelik, and F. Wilczek, Nucl. Phys. B **479**, 529 (1996).  
<sup>21</sup> A. Stern and B. I. Halperin, Phys. Rev. Lett. **96**, 016802 (2006).  
<sup>22</sup> P. Bonderson, A. Kitaev, and K. Shtengel, Phys. Rev. Lett. **96**, 016803 (2006).  
<sup>23</sup> E. Ardonne and E.-A. Kim, arXiv:0705.2902.  
<sup>24</sup> B. J. Overbosch and X.-G. Wen, arXiv:0706.4339.  
<sup>25</sup> W. Bishara and C. Nayak, Phys. Rev. B **77**, 165302 (2008).  
<sup>26</sup> X. Wan, K. Yang, and E. H. Rezayi, Phys. Rev. Lett. **97**, 256804 (2006).  
<sup>27</sup> S. H. Simon, E. H. Rezayi and N. R. Cooper, Phys. Rev. B. **75**, 195306 (2007); *ibid.* **75**, 075318 (2007); S. H. Simon, E. H.

Rezayi, N. R. Cooper, and I. Berdnikov, *ibid.* **75**, 075317 (2007).

<sup>28</sup> B. A. Bernevig and F. D. M. Haldane, arXiv:0711.3062.

<sup>29</sup> X. Wan, E. H. Rezayi, and K. Yang, Phys. Rev. B **68**, 125307 (2003).

<sup>30</sup> C. de C. Chamon and X. G. Wen, Phys. Rev. B **49**, 8227 (1994).

<sup>31</sup> B. I. Halperin, Helv. Phys. Acta. **56**, 75 (1983).

<sup>32</sup> Z.-X. Hu, X. Wan, and P. Schmitteckert, Phys. Rev. B **77**, 075331 (2008).

<sup>33</sup> Two  $+e/4$  quasiholes can form an alternative  $+e/2$  quasihole, which carries a neutral fermion (the  $\psi$  field from the Ising conformal field theory).<sup>8</sup> In the finite system, that state needs an odd number of electrons to realize due to a global constraint (not considered in this work). For even number of electrons, such a  $+e/2$  quasihole with a neutral fermion would require exciting an odd number of fermion modes at the edge.

<sup>34</sup> On a sphere, the counterpart of this wave function is

$$\text{Pf} \left( \frac{u_i v_j + u_j v_i}{u_i v_j - u_j v_i} \right) \prod_{i < j} (u_i v_j - u_j v_i)^2,$$

where  $(u, v)$  are the usual spinor coordinates.

<sup>35</sup> C. Tóke, N. Regnault, and J. K. Jain, Phys. Rev. Lett. **98**, 036806 (2006); arXiv:0707.0586.

<sup>36</sup> P. Fendley, M. P. A. Fisher, and C. Nayak, Phys. Rev. Lett. **97**, 036801 (2006); Phys. Rev. B **75**, 045317 (2007).

<sup>37</sup> J. J. Palacios and A. H. MacDonald, Phys. Rev. Lett. **76**, 118 (1996).

<sup>38</sup> X. Wan, K. Yang, and E. H. Rezayi, Phys. Rev. Lett. **88**, 056802 (2002).

<sup>39</sup> M. A. Cazalilla, N. Barberán, and N. R. Cooper, Phys. Rev. B **71**, 121303(R) (2005).

<sup>40</sup> A. E. Feiguin, E. H. Rezayi, C. Nayak, and S. Das Sarma, arXiv:0706:4469v2.

<sup>41</sup> Y. Yu, J. Phys.:Condens. Matter **19**, 621 (2007).

<sup>42</sup> K. Le Hur, Phys. Rev. B **65**, 233314 (2002); Phys. Rev. Lett. **95**, 076801 (2005); Phys. Rev. B **74**, 165104 (2006).

<sup>43</sup> J. S. Xia, W. Pan, C. L. Vicente, E. D. Adams, N. S. Sullivan, H. L. Stormer, D. C. Tsui, L. N. Pfeiffer, K. W. Baldwin, and K. W. West, Phys. Rev. Lett. **93**, 176809 (2004).

<sup>44</sup> M. Huber, M. Grayson, M. Rother, W. Biberacher, W. Wegscheider, and G. Abstreiter, Phys. Rev. Lett. **94**, 016805 (2005).

<sup>45</sup> S. Das Sarma, M. Freedman, C. Nayak, S. H. Simon, and A. Stern, arXiv:0707.1889v1.

<sup>46</sup> M. R. Peterson and S. Das Sarma, arXiv:0801.4819.